# UTILIZATION OF PHYSICAL FEATURES OF SCATTERED POWER FOR DEFECT CHARACTERIZATION

E. Domany
University of Washington
Seattle, Washington 98195

ABSTRACT

The first Born approximation provides a useful means to study scattering of ultrasound by various defects. In particular, it seems to yield qualitatively good results for the scattered power, when averaged over a range of frequencies. Features of the scattered power that have been discovered by this method will be reviewed. Closer study of some of these features leads to a step procedure to characterize an oblate spheroidal defect; to determine its orientation and shape. Procedures for extension to other shapes can also be given. Areas of future development will be indicated.

## Introduction

The first Born approximation provides a useful means to study scattering of ultrasound by various defects. In particular, it seems to yield qualitatively good results for the scattered power when averaged over a range of frequencies. Features of the scattered power that have been discovered by this method are reviewed. A convenient way to summarize the scattering data, by numerical projections, was used to assemble a library of scattered power from various defects. Addressing the particular problem of an oblate spheroidal cavity, a step-by-step procedure to determine its orientation and shape is suggested. Areas of future development are indicated.

I will discuss some features of elastic waves scattered by various defects, and try to outline a procedure to characterize the scatterer. Since this report is supposed to summarize a portion of a three-year effort, it should be remembered that two and a half years of my participation were at Cornell, and only the last five months at the University of Washington. Thus most of the results that I will list were obtained in collaboration with various present and past members of Jim Krumhansl's group.[1] The last part of my presentation (Procedure to Determine Orientation and Shape) deals with new developments. Thus some of what I will say has been presented before.

Let me briefly review the general philosophy of the approach we chose to take. We started out with very little understanding of the scattering of elastic waves. We were quickly impressed by the mathematical complexity of the problem. The basic situation is depicted in Fig. 1; an incident elastic wave scattered by a defect. Exact solutions to this problem are available only for a limited class of scatterers. For scatterers of finite volume, only the spherical defect is soluble! Since deviations from spherical geometry were an important aspect of the program, we decided to consider various approximate treatments. The idea was to check the approximations against theory and experiment, and try to use them to provide us with some qualitative insight into the scattering mechanism.

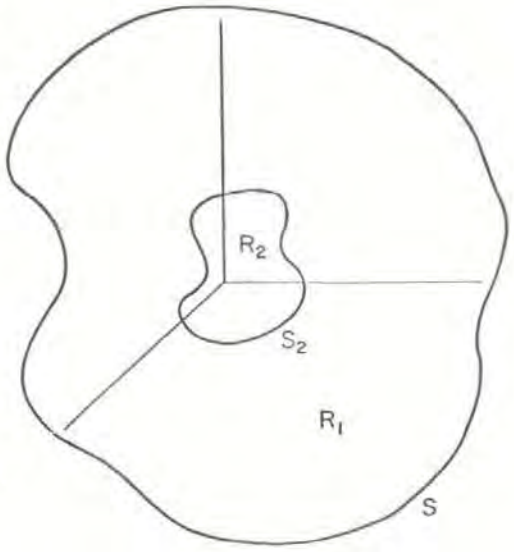


$R = R_1 + R_2$
$S_1 = S + S_2$

Figure 1. The basic scattering situation, with scatterer R.

We hoped to characterize a general defect by an effective ellipsoid. Thus we were led to consider the simplest ellipsoid, i.e., a spheroidal cavity. Although we did concentrate on this object, we have also looked at cylindrical defects, prolate spheroids, and more recently extended our study to various cracks. The methods used were based mainly on the Born approximation,[2] and later on a quasi-static approximation.[3]

Our main concern was to try to isolate a few qualitative features, present those to experimentalists, and urge them to verify or discard them. We have benefited from those interactions, especially with Dr. B. Tittmann and Dr. L. Adler.

Another aspect I should mention was our collaboration with Dr. A. Mucciardi and R. Shankar of Adaptronics, whom we supplied with the Born approximation program to help train their computer.[4]

The structure of this report is as follows. In the discussion of "Physical Features of the Scattered Fields," a step-by-step procedure to characterize an oblate spheroidal cavity is presented. The second on "Areas of Future Development and Summary" summarizes and indicates areas of future development.

## Physical Features of the Scattered Fields

By comparing the BA results with the exact solutions, we saw that for cavities the BA has a chance of being useful mainly in the backscattered regime. We also noticed that the BA misses the detailed frequency dependence of the scattered power, and does not contain any phase information. Thus we are led to consider the angular distribution of frequency averaged power.

Consider a scatterer characterized by two lengths, a,b (an oblate spheroid of width 2a and radius b is an example, but similar considerations hold for cylinders and "flat" objects of more general shape). Choose the axis a (the symmetry axis of the spheroid) as the direction of incidence of longitudinal waves. Within the integral equation formulation,[2,3] the defect is the source of the scattered waves. When viewed along the a-axis, an area $\sim b^2$ of the source is seen; while when viewed from the side (at 90° to the a axis) the area is $\sim ab$. Thus the ratio $R_1 = P_{180}/P_{90}$ of the backscattered frequency averaged power to that scattered at 90° is expected to increase with increasing b/a (or "flatness"). This qualitative picture was obtained by analyzing the results of the Born approximation for various scatterers. Within the approximation this behavior is predicted to hold quite independently of the detailed shape (i.e., for cylinders as well as spheroids). Experimentally,[5] it was checked for spheroids only - comparison of experiment and the Born approximation prediction is given in Fig. 2.

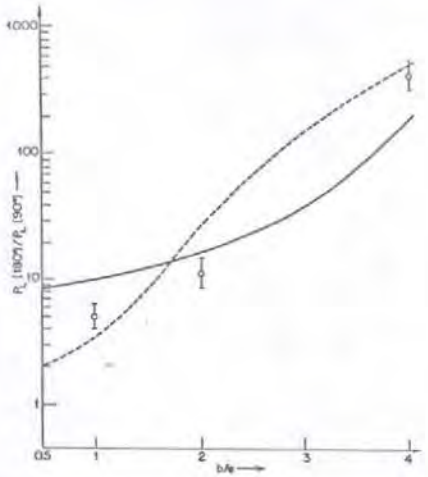


Figure 2. The ratio P(180)/P(90) for longitudinal power with longitudinal wave incident along symmetry axis of spheroidal cavities in Ti, vs. b/a of the scatterer. Uniform averages of 0<ka<1 (full lines) and 9<ka<2 (broken lines) were used. The circles are experimental results.

The experimental procedure involved in measuring this feature is a two transducer (pitch-catch) mode. An alternative mode of operation uses a single transducer (pulse-echo). This mode is useful to investigate the dependence of backscattered power on the angle of incidence. Obviously, for a spherical scatterer there is no preferred direction, and the backscattered power is independent of the direction of incidence. For a flat object, however, we expect more backscatter when the incidence is along the a-axis, than when along the b-axis. Thus, a variation of the backscattered power with angle of incidence, α, is another measure of the b/a ratio. Experiment and theory are compared on Fig. 3. On Fig. 4 we plot $R_2 = P_{180}(\alpha=0)/P_{180}(\alpha=90)$ as a function of b/a, for various spheroids.

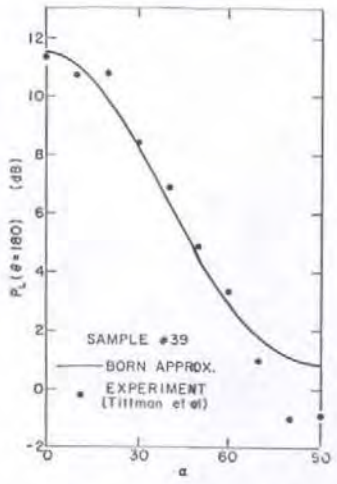


Figure 3. Backscattered longitudinal power $P_L$ ($\theta=180°$), as a function of angle of incidence, α, for spheroidal cavity ($b=400\mu$, $a=200\mu$) in titanium. Rockwell transducer characteristics were used for the frequency averaging. The line is the Born approximation; dots are measurements (Tittmann, et al.).

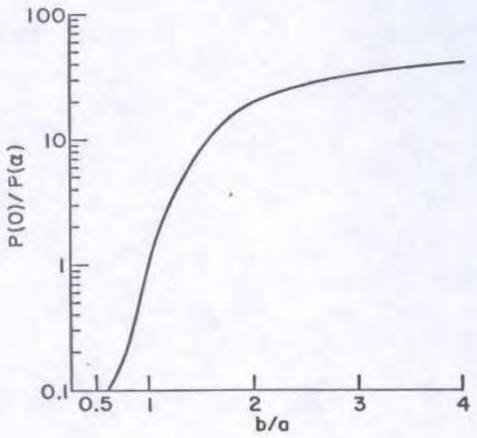


Figure 4. Ratio of backscattered power at $\alpha = 0$ and $\alpha = 90^{\circ}$, vs. b/a, for spheroidal cavities in titanium: Born approximation.

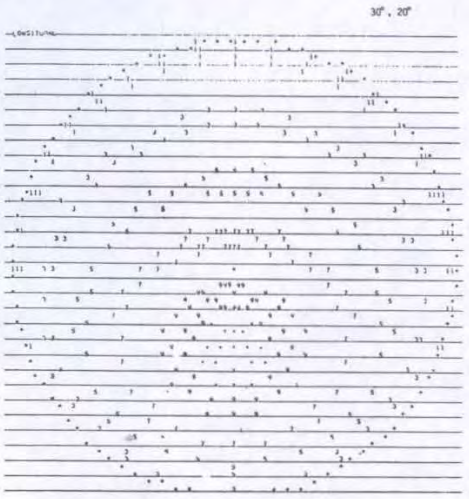

Figure 5. Projection map of frequency averaged longitudinal power. The transmitter is at the center of the circle, the perimeter corresponds to scattering at $90^{\circ}$. The defect is an oblate spheroid with b/a = 2, oriented at $\alpha = 30^{\circ}$ ($\alpha$ is the angle between the incident wave and the symmetry axis of the spheroid).

Both kinds of operational modes are most conveniently summarized in intensity projection maps. Figure 5 is an example of a pitch-catch mode experiment, and Fig. 6 is the same for a pulse-echo mode. In both cases the circle is the projection of an experimentally accessible "window." In Fig. 5 the source is at the center of the window, and the numbers represent the frequency averaged power scattered to a transducer whose position is projected to the plane of the figure. In Fig. 6 all numbers represent backscattered power to various transducer positions. We have compiled an extensive library of such projection maps for various spheroidal defect shapes and orientations (with respect to the window). Such a library may prove useful to decide on experiments and their interpretation, and also in suggesting an inversion procedure. One simple but important feature of these maps is the existence of a line of symmetry, which will be discussed and utilized in the inversion procedure discussed in the section on "Procedure to Determine Orientation and Shape." Although such a line of exact symmetry is a property of an object with an axis of rotational symmetry, a more general shaped object will possess a best line of approximate symmetry, which can be instrumental in modeling the defect by an effective spheroid.

Figure 6. Same scatterer as Fig. 5; each number represents the backscattered power to a transducer operated in pulse-echo mode.

## Procedure to Determine Orientation and Shape

Here we narrowed our attention to oblate spheroidal defects, viewed in a "window" of a 60° cone.

The geometry of the window and the defect is shown in Fig. 7. Since the same problem was treated by Mucciardi et al.[4] using an adaptive learning procedure, it seems appropriate to emphasize the difference between the two approaches. In the adaptive method one or more sets of measurements taken within the accessible window are analyzed in an empirical way. This approach aims at taking a fixed set of measurements, and performing the analysis after these were taken.

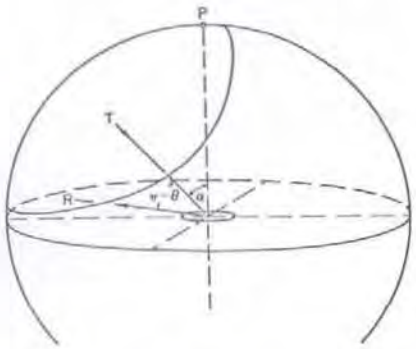


Figure 7. Geometry of experimental setup used to determine line of symmetry. The transmitter, T, is at the center of the window; α is the angle between the direction of incidence and the symmetry axis of the defect. This axis intersects the window at P. R is position of receiver, θ is the scattering angle. To determine the orientation we want to locate P. The line of symmetry connects P and T.

In contradistinction, the approach I follow is more interactive in character: the first set of measurements is analyzed, and the results of this analysis determine which second set of measurements to take. Since the analysis turns out to be quite simple, it is hoped that it can be performed "on line," and the resulting optimization of further measurements to be made compensates in terms of time and expenses.

The shortcoming of this approach is that it is harder to verify directly at this stage, since it requires closer interaction between analysis and experiment. One cannot take a complete set of measurements and assign them to analysis as a "homework exercise." Let us proceed now to outline the procedure step by step.

Orientation - (Step 1) When the central transducer of the array is used as the source, the scattered power is symmetric about the plane defined by the direction of the incident power and the symmetry axis (Fig. 1). We considered three sets of measurements taken by B. Tittmann, and tried to determine the plane of symmetry by a best-fit method based on three Legendre polynomials.[6] In two cases we were able to determine the symmetry plane to within 2°; in case 3 to within 20°. Note that this is not a check on theory, but rather on experimental accuracy. I would conclude that improved analysis (taking measurement errors into account) will provide a scheme to determine the line of symmetry to within 5-10°. Since this line runs through the center of our array and the symmetry axis of the defect, we can proceed to find the exact location of the axis.

(Step 2) Having found the line that contains the symmetry axis, we proceed utilizing one of the features that were discussed previously in "Physical Features of the Scattered Fields." We operate transducers in the pulse-echo mode along this line. Plotting backscattered power vs. positions, we get a curve like Fig. 3. The window specification is such that we either have access to both the major and minor axes, or at least to one of them. Thus the measured curve will exhibit either both a minimum and maximum, or one of these. In any case it is sufficient to pin down the orientation of the defect.

Shape and Size - I have tried to use various features of the scattered power to determine shape and size. This, however, seems to be a hard problem: we need two features at least to determine the two unknowns (b/a and absolute size). Various pairs of features that I considered did not provide sufficient resolution to make possible a reliable determination for any arbitrary position of the experimentally accessible window. If we have a reasonable estimate of the absolute size, using features from Fig. 2 or 4, b/a will be determined. But when both absolute size and b/a are unknown, the geometrical restriction and experimental error make a simultaneous determination of both quite unreliable (i.e., with large uncertainty).

However, seeing some of Bernie Tittmann's data, a most intriguing possibility emerged.[7] Consider the two curves in Fig. 8. These are backscattered amplitudes vs. frequency, taken at two angles of incidence, $\alpha = 0$ and $\alpha = 60°$, $A_0(f)$ and $A_{60}(f)$.

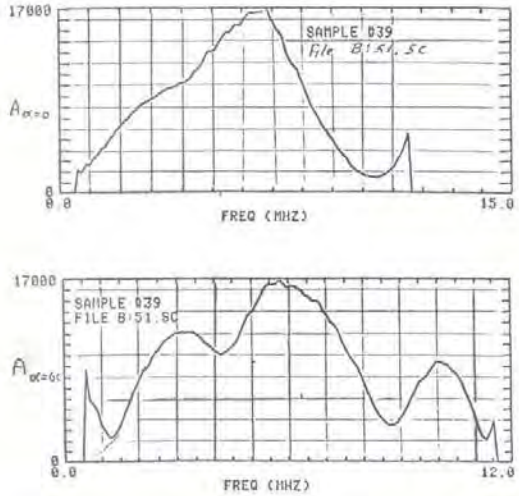


Figure 8. Amplitude vs. frequency of backscattered wave from oblate spheroid (b = 400μ, a = 200μ) in Ti, for angle of incidence $\alpha = 0°$, and $\alpha = 60°$.

We can now plot $A_0$ vs. $A_{60}$, using f as a parameter (see Fig. 9). This way we produce a universal curve for a spheroid of a given shape (i.e., b/a). Absolute size will determine only how far, for a given transducer, we can trace the curve. Note that for a sphere we obtain the straight line $A_0 = A_{60}$. Similar analysis of phase information will make this method even more powerful. Again, this prediction is independent of any approximation.

For comparison, we presented a similar plot for a spheroid of large b/a ratio. Clearly, the extent of deviations from a straight line is different: thus we can use these curves to predict b/a, and then from the length of the curve obtain the absolute size.

## Areas of Future Development and Summary

As indicated by the last section, development of approximations that yield reliable frequency and phase information seem to be the most important issue at hand; although development of sophisticated inversion schemes based on currently available approximations does seem to be fruitful, I believe that the inversion problem will also be much simplified if one has a good handle on frequency and phase information.

Approximations with this aim in mind are currently developed,[10] and will be discussed by others. My main effort will be directed towards developing the distorted wave Born approximation, utilizing the exact solution for spheres to study scattering by ellipsoidal defects.

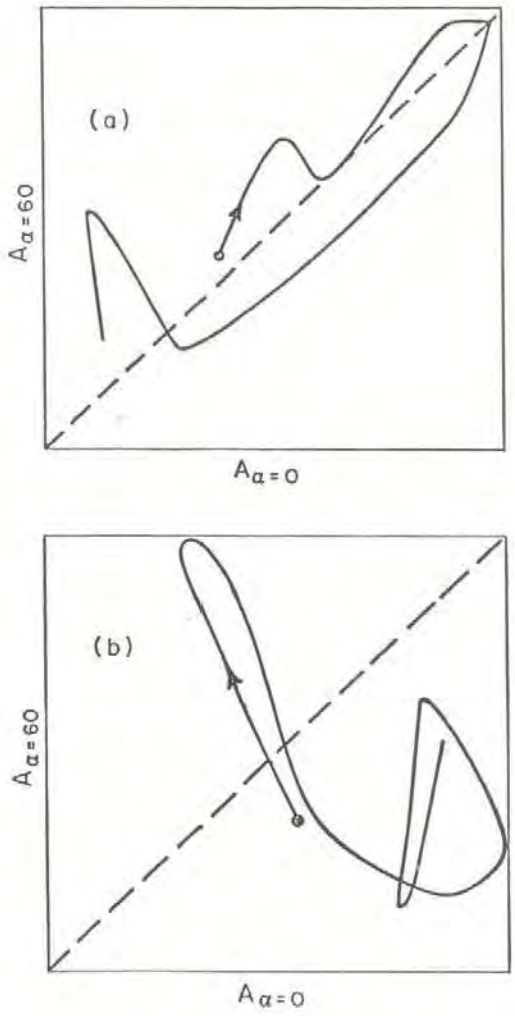


Figure 9. Plot of equally normalized amplitude, $A_{60}(f)$ vs. $A_0(f)$, using the frequency f as a parameter. The heavy dot indicates f = 2 MHz, and the arrow the direction of increasing f. The dashed line is the expected curve for a spherical defect.

(a) b = 400μ, a = 200μ
(b) b = 400μ, a = 100μ

## Acknowledgements

I have greatly benefited from advice and encouragement from J. A. Krumhansl, J. E. Gubernatis, D. O. Thompson, B. Thompson, L. Adler and many others. I enjoyed a particularly pleasant and fruitful interaction with B. Tittmann, whose experiments provided both stimulus and insight, and shaped my approach to the problem. B. Delaplain helped me in developing and programming the best fit analysis of the symmetry line.

This research was sponsored by the Center for Advanced NDE operated by the Science Center, Rockwell International, for the Advanced Research Projects Agency and the Air Force Materials Laboratory under contract F33615-74-C-5180.

## References

1. J. A. Krumhansl, E. Domany, J. E. Gubernatis, P. Muziku, S. Teitel, D. Wood, Interdisciplinary Program for Quantitative Flaw Definition, Special Report Second Year Effort, p. 102.

2. J. E. Gubernatis et al., J. Appl. Phys., to be published.

3. See J. E. Gubernatis, this report.

4. R. Shankar, A. N. Mucciardi, M. F. Whalen, and M. D. Johnson, this report.

5. The experiments quoted here and elsewhere in this report were performed by B. R. Tittmann and R. K. Elsley, Science Center, Rockwell International; see this report and references therein.

6. B. Delaplain and E. Domany, unpublished.

7. E. Domany and B. R. Tittmann, to be published.

8. N. Bleistein and J. K. Cohen, this report.

9. J. Rose and J. A. Krumhansl, to be published.

10. Y. H. Pao, previous work; Y. H. Pao and V. Varadan, "Proceedings, ARPA/AFML Review of Progress in Quantitative NDE," Cornell University, June 14-17, 1977, and references therein (to be published).